



waterscales



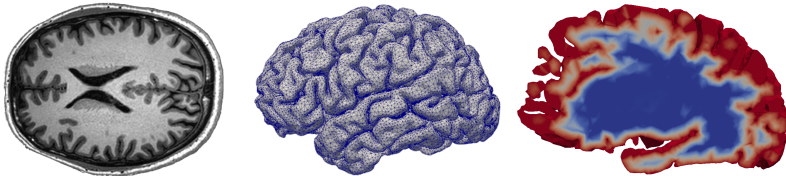
## Brain modelling: from magnetic resonance images to finite element simulation

Marie E. Rognes

Oslo, Norway

Jan 15, 22, and 29 2021

# Outline of lectures



Lectures 1-2 Quick start: From brain MRI to FEM

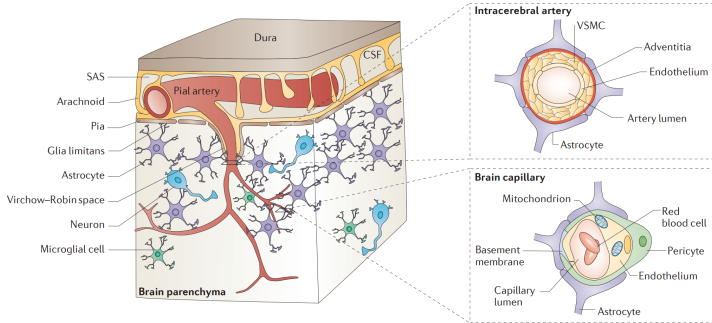
Lectures 3-4 The poroelastic brain

- I The brain as a poroelastic medium: properties and forces
- II Models and numerics for the poroelastic brain at the macroscale
- III From hemispheres to brain meshes and simulations

Lectures 5-6 Introducing diffusion tensor images (anisotropy, parcellations)

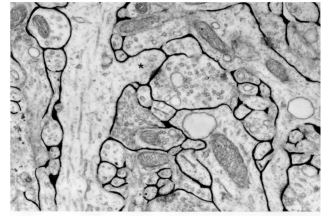
## I: The brain as a poroelastic medium

# At the macroscale, the brain can be viewed as an elastic medium permeated by multiple fluid-filled networks



The brain parenchyma includes multiple fluid networks (extracellular spaces (ECSs), arteries, capillaries, veins, paravascular spaces (PVSs))

[Zlokovic (2011)]



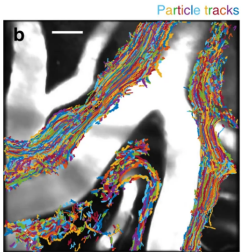
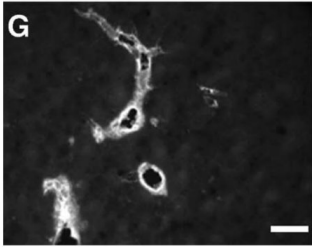
Rat cerebral cortex with ECS in black  
(Scale bar:  $\approx 1\mu\text{m}$ )

[Nicholson (2001) (Fig. 2)]

**The brain is ( $\approx$ ):**  
5-10% blood  
20% ECS  
70-75% brain cells  
80% water

[Budday et al (2019)]

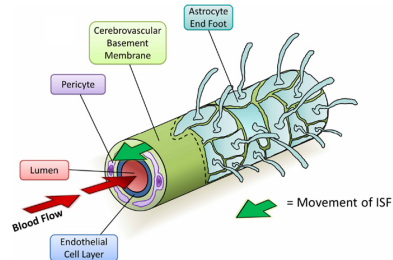
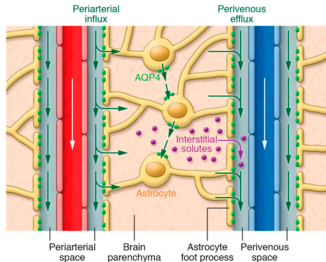
# Fluid movement in perivascular spaces enhances solute transport



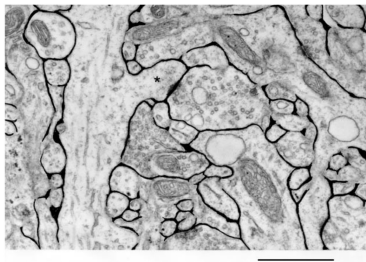
**Key mechanism** for brain solute transport: CSF/ISF flow in perivascular spaces – interacting with extra/intracellular water movement.

**Open questions** Existence? Directionality? Magnitude? Anatomy? Importance?

[Hadaczek et al (2005) (Fig 2), Kaur et al (2020), Iliff et al (2012), Morris et al (2014), Mestre et al (2018) (Fig 1) etc.]



# Solutes can diffuse in the narrow and tortuous extracellular spaces



Rat cerebral cortex with ECS in black (Scale bar:  $\approx 1\mu\text{m}$ )

[Nicholson (2001) (Fig. 2); Holter et al (2017) (Fig. 1)]

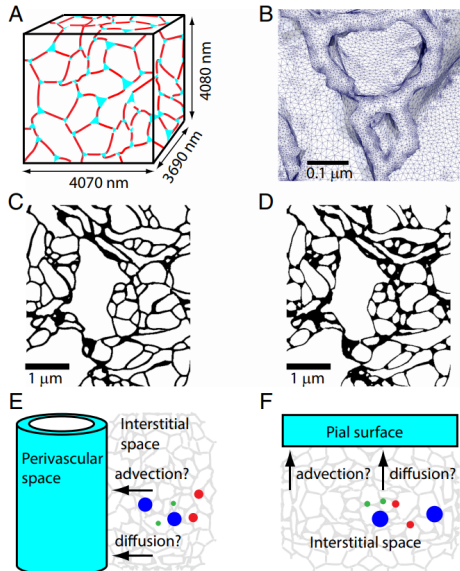
**ECS diffusion and tortuosity**  $D^* = D\lambda^{-2}$ :

Nicholson (2001):  $\lambda \approx 1.6$

**ECS permeability** ( $\kappa$ ,  $\text{nm}^2$ ):

Holter et al (2017): 10-20

Basser (1992): 4000



# Brain tissue is soft, heterogeneous and rheologically complex

## Brain tissue is

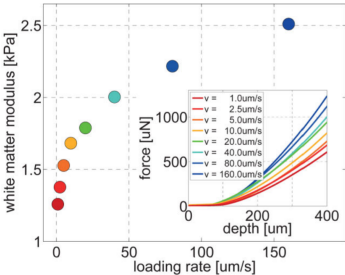
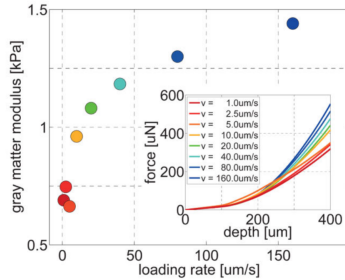
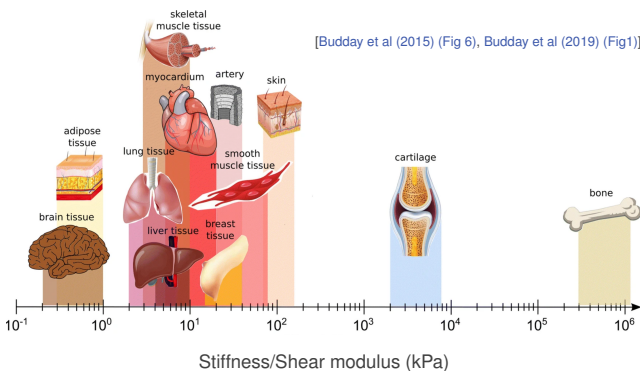
soft (shear modulus  $\approx 0.5\text{--}2.5\text{ kPa}$ )

stiffer with increasing strain/strain rates (nonlinear)

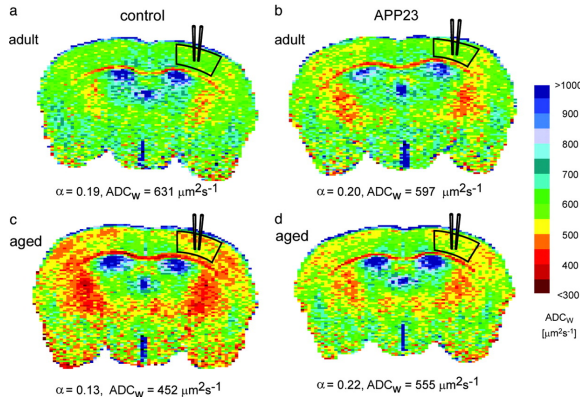
stiffer during loading than unloading (viscoelastic)

stiffer in compression than in tension (poroelastic)

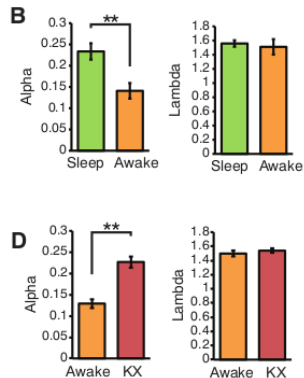
stiffer in some regions than in others (heterogeneous)



# Brain tissue is active and dynamic, and its properties change with circadian rhythm, age and pathologies



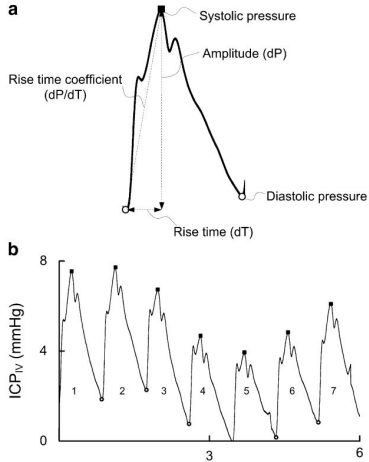
Volume fractions  $\alpha$  and apparent diffusion coefficients (ADC) in aging and Alzheimer's disease model mouse (APP23) ([Sykova et al \(2005\)](#) (Fig 2)).



Volume fractions  $\alpha$  and tortuosity  $\lambda$  in sleeping, anaesthetized (KX) and awake mice ([Xie et al., Science, 2013](#)).

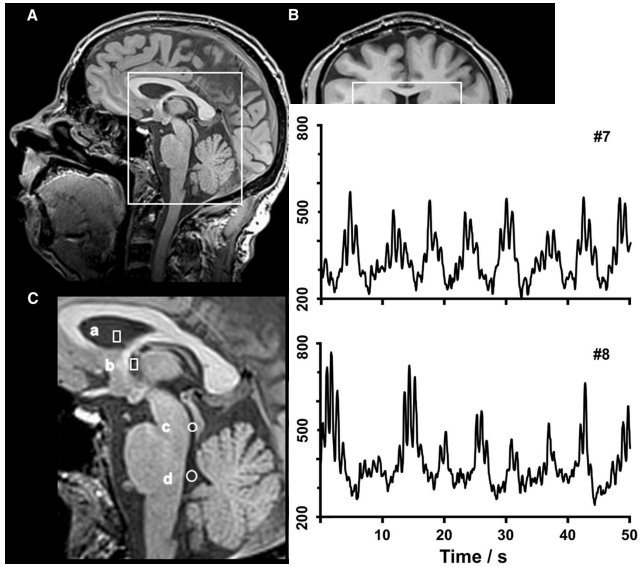
## I: What do we know of the forces at play?

# Intracranial pressure (ICP) pulsates and CSF flow oscillates

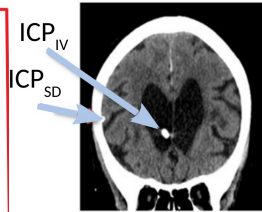
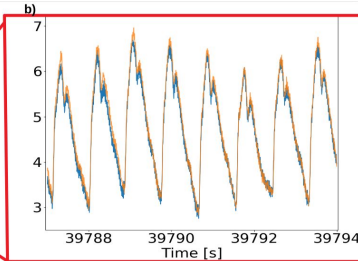
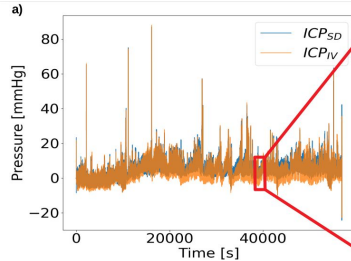


[Eide and Sæhle (2010)]

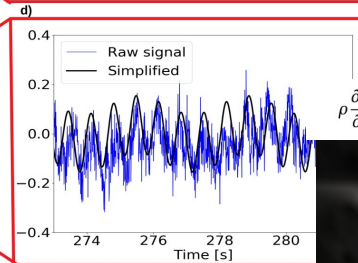
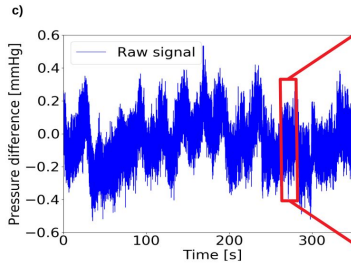
[Dreha-Kulaczewski et al, (2015)]



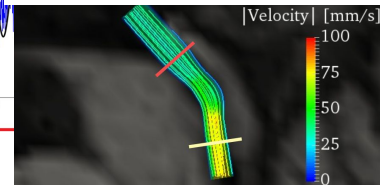
# ICP differences in time (4-10 mmHg) and space ( $\leq 0.2$ mmHg)



Long term ICP measurements

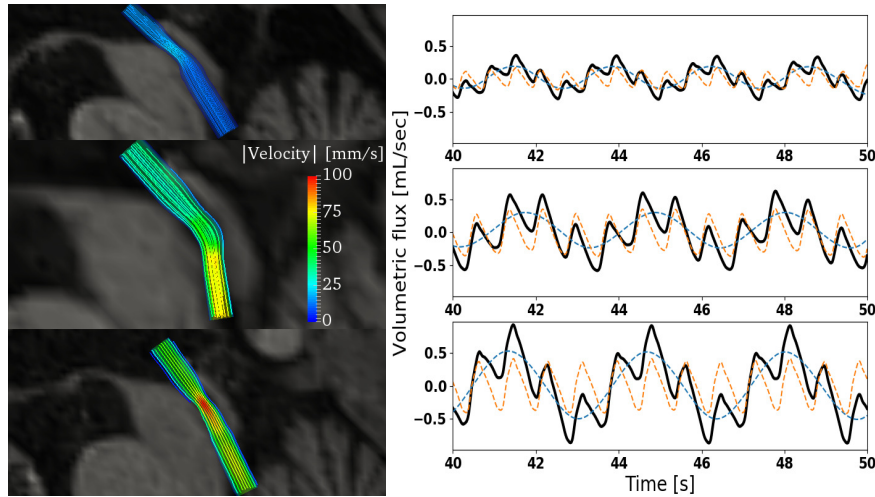


$$\rho \frac{\partial v}{\partial t}(r, t) - \frac{\mu}{r} \frac{\partial v}{\partial r}(r, t) - \mu \frac{\partial^2 v}{\partial r^2}(r, t) = -\frac{dp}{dz}(t).$$



[Vinje et al, *Scientific Reports*, 2019]

Intracranial pressure gradients are dominated by the cardiac cycle, but can induce respiration-dominated CSF flow volumes



[Vinje et al (2019)]

# Intracranial dynamics result from an interplay between arterial blood influx, cerebrospinal fluid flow, venous outflux, and compliances

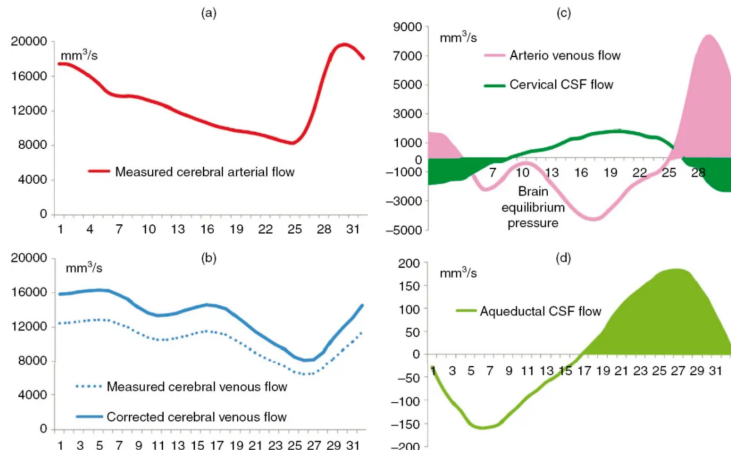
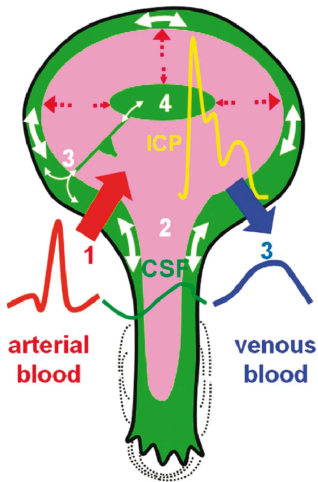


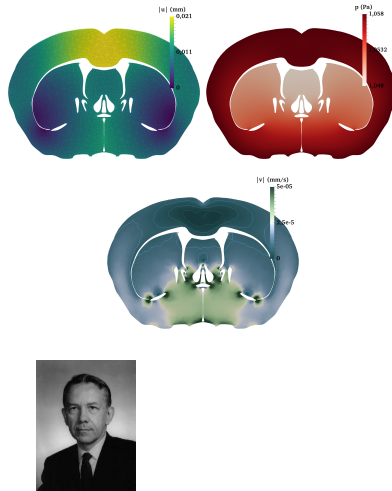
Figure 12.4 CSF and cerebral blood flow during the cardiac cycle in healthy adults (see text for full explanation).

## **II: Porous media brain modelling**

# Biot's equations describe displacement and fluid pressure in a poroelastic medium

Find the displacement  $u = u(x, t)$  and the pressure  $p = p(x, t)$  over  $\Omega \times [0, T]$  such that:

$$\begin{aligned} -\operatorname{div}(2\mu\varepsilon(u) + \lambda \operatorname{div} u I - pI) &= f, \\ c_0 \dot{p} + \operatorname{div} \dot{u} - \operatorname{div} K \operatorname{grad} p &= g \end{aligned}$$



[Biot (1941), Murad, Thomée and Loula (1992-1996), Phillips and Wheeler (2007-2008), and many others]

# Biot's equations describe displacement and fluid pressure in a poroelastic medium

Find the displacement  $u = u(x, t)$  and the pressure  $p = p(x, t)$  over  $\Omega \times [0, T]$  such that:

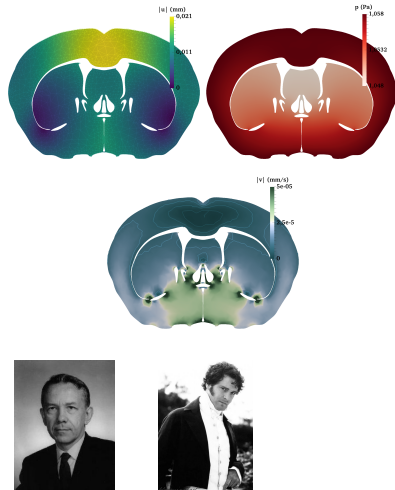
$$-\operatorname{div}(2\mu\varepsilon(u) + \lambda \operatorname{div} u I - pI) = f,$$

$$c_0 \dot{p} + \operatorname{div} \dot{u} - \operatorname{div} K \operatorname{grad} p = g$$

**Low-storage, incompressible regime:**  $c_0 = 0, \lambda \rightarrow \infty$ :  
 $\operatorname{div} u \rightarrow 0$ , system decouples

$$-\operatorname{div} K \operatorname{grad} p = g \quad (\text{Darcy})$$

$$-\operatorname{div}(2\mu\varepsilon(u) + \lambda \operatorname{div} u) = f - \operatorname{grad} p \quad (\text{Elasticity})$$



# Biot's equations describe displacement and fluid pressure in a poroelastic medium

Find the displacement  $u = u(x, t)$  and the pressure  $p = p(x, t)$  over  $\Omega \times [0, T]$  such that:

$$-\operatorname{div}(2\mu\varepsilon(u) + \lambda \operatorname{div} u I - pI) = f,$$

$$c_0 \dot{p} + \operatorname{div} \dot{u} - \operatorname{div} K \operatorname{grad} p = g$$

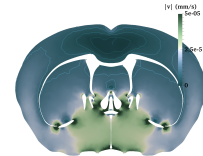
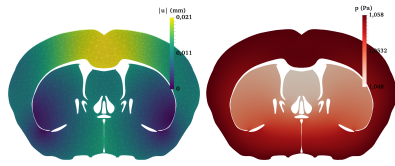
**Low-storage, incompressible regime:**  $c_0 = 0, \lambda \rightarrow \infty$ :  
 $\operatorname{div} u \rightarrow 0$ , system decouples

$$-\operatorname{div} K \operatorname{grad} p = g \quad (\text{Darcy})$$

$$-\operatorname{div}(2\mu\varepsilon(u) + \lambda \operatorname{div} u) = f - \operatorname{grad} p \quad (\text{Elasticity})$$

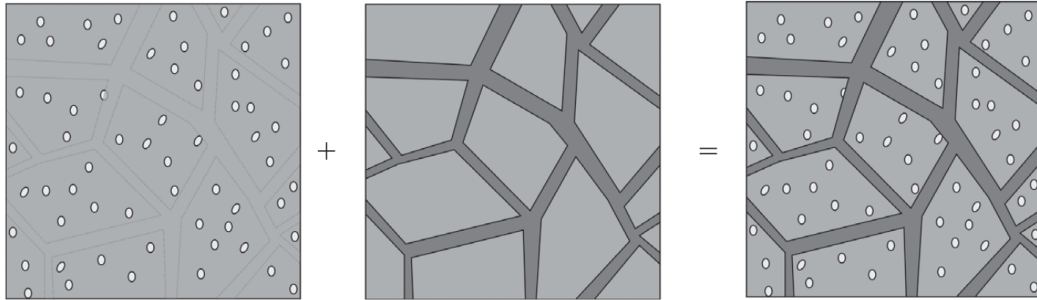
**Low-storage, impermeable regime:**  $c_0 = 0, K \rightarrow 0$ :

$$-\operatorname{div}(2\mu\varepsilon(u) + \lambda \operatorname{div} u - pI) = f, \quad (\text{Stokes})$$
$$\operatorname{div} u = 0$$



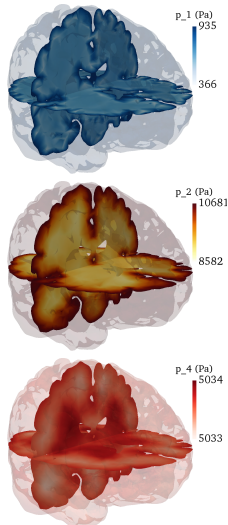
[Biot (1941), Murad, Thomée and Loula (1992-1996), Phillips and Wheeler (2007-2008), and many others]

Multiple-network poroelastic theory (MPET) is a macroscopic model for poroelastic media with multiple fluid networks



[Bai, Elsworth, Roegiers (1993); Tully and Ventikos (2011)]

# The multiple-network poroelasticity (MPET) equations describe displacement and fluid pressures in generalized poroelastic media



Find the displacement  $u = u(x, t)$  and  $J$  (network) pressures  $p_j = p_j(x, t)$  for  $j = 1, \dots, J$  such that

$$\begin{aligned} -\operatorname{div}(2\mu\varepsilon(u) + \lambda \operatorname{div} u \mathbf{I} - \sum_j \alpha_j p_j \mathbf{I}) &= f, \\ c_j \dot{p}_j + \alpha_j \operatorname{div} \dot{u} - \operatorname{div} K_j \operatorname{grad} p_j + S_j &= g_j \quad j = 1, \dots, J. \end{aligned}$$

Fluid exchange between networks:

$$S_j = \sum_i s_{i \leftarrow j} = \sum_i \xi_{j \leftarrow i} (p_j - p_i).$$

$J = 1$  corresponds to Biot's equations,  $J = 2$  Barenblatt-Biot.  
 $\lambda \rightarrow \infty$ ,  $c_j \rightarrow 0$ ,  $\xi_{j \leftarrow i} \gg 1$ ,  $\xi_{j \leftarrow i} \ll 1$  and  $K \rightarrow 0$  interesting regimes.

[Biot, 1941; Bai, Elsworth and Roegiers, Water Resources Research, 1993]

[Tully and Ventikos, Jour Fluid Mech., 2011; Lee, Piersanti, Mardal, R., SISC, 2019]

## **II: Finite element methods for generalized poroelasticity**

## Deriving a finite element formulation for the MPET equations (I)

$$\begin{aligned} -\operatorname{div}(2\mu\varepsilon(u) + \lambda \operatorname{div} u \mathbf{I} - \sum_j \alpha_j p_j \mathbf{I}) &= f, \\ c_j \dot{p}_j + \alpha_j \operatorname{div} \dot{u} - \operatorname{div} K_j \operatorname{grad} p_j + S_j &= g_j \quad j = 1, \dots, J, \end{aligned}$$

where

$$S_j = \sum_i \xi_{j \leftarrow i} (p_j - p_i).$$

## Deriving a finite element formulation for the MPET equations (II)

# Introducing notation for variational formulations

Boundary conditions:

Initial conditions

$L^2$ -inner product and norm (with weights)

$V$

$Q_0$

$Q_1, \dots, Q_J$

## Standard finite element formulation is not robust for incompressible materials ( $\lambda \rightarrow \infty$ )

Standard Taylor-Hood  $(u_h, p_h) \in \mathcal{P}_2^d \times \mathcal{P}_1^A$  discretization in space:

$$\langle 2\mu\varepsilon(u), \varepsilon(v) \rangle + \langle \lambda \operatorname{div}(u), \operatorname{div}(v) \rangle - \sum_j \langle \alpha_j p_j, \operatorname{div} v \rangle = \langle f, v \rangle \quad \forall v \in V_h,$$

$$\langle c_j \dot{p}_j + \alpha_j \operatorname{div} \dot{u} + S_j, q_j \rangle + \langle K_j \operatorname{grad} p_j, \operatorname{grad} q_j \rangle = \langle g_j, q_j \rangle \quad \forall q_j \in Q_{j,h} \quad j = 1, \dots, J,$$

E.g. Crank-Nicolson discretization in time.

Loss of convergence even for smooth example (Test case A [Yi (2017)]) with moderate  $\lambda$ :  
 $J = 2, \mu = 1/3, \lambda = 5/3 \times 10^4$ .

$P_2^2 \times P_1 \times P_1$	$\ u - u_h(T)\ $	Rate	$\ u - u_h(T)\ _1$	Rate
$h$	0.169		2.066	
$h/2$	0.040	2.09	0.980	1.08
$h/4$	0.010	2.04	0.480	1.03
$h/8$	0.002	2.03	0.235	1.03
$h/16$	0.001	2.09	0.110	1.10
Optimal		3		2

## Introducing the total pressure $p_0$ as an additional variable for MPET

Key idea: inspired by [Lee, Mardal, Winther, 2017]: introduce the total pressure

$$p_0 = \lambda \operatorname{div} u - \sum_{j=1}^J \alpha_j p_j \leftrightarrow \operatorname{div} u = \lambda^{-1} \alpha \cdot p$$

with  $\alpha = (1, \alpha_1, \dots, \alpha_J)$ ,  $p = (p_0, \dots, p_J)$ .

## Introducing the total pressure $p_0$ as an additional variable for MPET

Key idea: inspired by [Lee, Mardal, Winther, 2017]: introduce the total pressure

$$p_0 = \lambda \operatorname{div} u - \sum_{j=1}^J \alpha_j p_j \leftrightarrow \operatorname{div} u = \lambda^{-1} \alpha \cdot p$$

with  $\alpha = (1, \alpha_1, \dots, \alpha_J)$ ,  $p = (p_0, \dots, p_J)$ .

### Total-pressure formulation of the MPET equations

Given (compatible)  $u^0$  and  $p_i^0$ ,  $f$  and  $g_i$  for  $i = 1, \dots, J$ , find  $u \in H^1((0, T]; V)$  and  $p_j \in H^1((0, T]; Q_j)$  for  $j = 0, \dots, J$  such that

$$\langle 2\mu\varepsilon(u), \varepsilon(v) \rangle + \langle p_0, \operatorname{div} v \rangle = \langle f, v \rangle$$

$$\langle \operatorname{div} u, q_0 \rangle - \langle \lambda^{-1} \alpha \cdot p, q_0 \rangle = 0$$

$$\langle c_j \dot{p}_j + \alpha_j \lambda^{-1} \alpha \cdot \dot{p} + S_j, q_j \rangle + \langle K_j \operatorname{grad} p_j, \operatorname{grad} q_j \rangle = \langle g_j, q_j \rangle, \quad j = 1, \dots, J,$$

for all  $v \in V$  and  $q_j \in Q_j$ .

[Lee, Piersanti, Mardal, R., SISC, (2019)]

# Introducing the total pressure $p_0$ as an additional variable for MPET

Key idea: inspired by [Lee, Mardal, Winther, 2017]: introduce the total pressure

$$p_0 = \lambda \operatorname{div} u - \sum_{j=1}^J \alpha_j p_j \leftrightarrow \operatorname{div} u = \lambda^{-1} \alpha \cdot p$$

with  $\alpha = (1, \alpha_1, \dots, \alpha_J)$ ,  $p = (p_0, \dots, p_J)$ .

## Total-pressure formulation of the MPET equations

Given (compatible)  $u^0$  and  $p_i^0$ ,  $f$  and  $g_i$  for  $i = 1, \dots, J$ , find  $u \in H^1((0, T]; V)$  and  $p_j \in H^1((0, T]; Q_j)$  for  $j = 0, \dots, J$  such that

$$\langle 2\mu\varepsilon(u), \varepsilon(v) \rangle + \langle p_0, \operatorname{div} v \rangle = \langle f, v \rangle$$

$$\langle \operatorname{div} u, q_0 \rangle - \langle \lambda^{-1} \alpha \cdot p, q_0 \rangle = 0$$

$$\langle c_j \dot{p}_j + \alpha_j \lambda^{-1} \alpha \cdot \dot{p} + S_j, q_j \rangle + \langle K_j \operatorname{grad} p_j, \operatorname{grad} q_j \rangle = \langle g_j, q_j \rangle, \quad j = 1, \dots, J,$$

for all  $v \in V$  and  $q_j \in Q_j$ .

[Lee, Piersanti, Mardal, R., SISC, (2019)]

## Theorem (Energy estimate for quasi-static multiple-network poroelasticity)

Assume that  $u \in C^1([0, T]; V)$  and  $p_j \in C^1([0, T]; Q_j)$  for  $j = 0, \dots, J$  are solutions of the total pressure formulation of the quasi-static MPET equations. Then, for all  $t \in (0, T]$ , and uniformly in  $\lambda \gg 0$  and  $c_j$  for  $j = 1, 2, \dots, J$

$$\begin{aligned} \|\varepsilon(u(t))\|_{2\mu}^2 + \sum_{j=1}^J \|p_j(t)\|_{c_j}^2 + \|p_0(t)\|^2 + \int_0^t \sum_{j=1}^J \|\operatorname{grad} p_j(s)\|_{K_j}^2 ds \\ \lesssim I_0^2 + \|\dot{f}\|_{L^1(0, T; L^2)}^2 + \|f(t)\|^2 + \sum_{j=1}^J \|g_j\|_{L^2(0, T; L^2)}^2, \end{aligned}$$

where  $I_0 = \|\varepsilon(u(0))\|_{2\mu} + \sum_{j=1}^J \|p_j(0)\|_{c_j} + \|\alpha \cdot p(0)\|_{\lambda^{-1}} + \|f(0)\|$ .

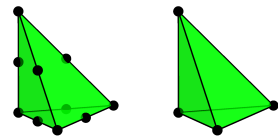
### Proof.

Standard techniques, summing with  $v = \dot{u}$ ,  $q_j = p_j$  for  $j = 1, \dots, J$ ,  $q_0 = -p_0$  in time-derivative of 2nd eq., combined with improved Grönwall-type estimate. Estimate for  $p_0$  follows from inf-sup condition. □

[Thm 3.3., Lee, Piersanti, Mardal, R., 2019]

# Introducing compatible finite element semi-discretization(s)

Let  $\mathcal{T}_h$  denote a conforming, shape-regular, simplicial discretization of  $\Omega$  with discretization size  $h > 0$ . Relative to  $\mathcal{T}_h$ , we define finite element spaces  $V_h \subset V$  and  $Q_{j,h} \subset Q_j$  for  $j = 0, \dots, J$ .



Assume that

- A1:**  $V_h \times Q_{0,h}$  is a stable (in the Brezzi sense) finite element pair for the Stokes equations;
- A2:**  $Q_{j,h}$  is Poisson-convergent finite element of polynomial order  $l_j$  for  $j = 1, \dots, J$ .

Denote  $Q_h = Q_{0,h} \times Q_{1,h} \times \dots, Q_{J,h}$ .

These two assumptions are fulfilled by for instance:

- $V_h \times Q_h = \mathcal{P}_{l+1}(\mathcal{T}_h) \times \mathcal{P}_l^{J+1}(\mathcal{T}_h)$  for  $l = 1, 2, \dots$ , (Taylor-Hood-type elements).

Define the **semi-discrete formulation(s)** by searching for  $u_h, p_{j,h}$  satisfying the total pressure formulation of the MPET equations over  $V_h$  and  $Q_{j,h}$  for  $j = 0, \dots, J$ .

# Introducing Stokes-type and weighted elliptic-type projections as auxiliary interpolation operators

For any  $(u, p_0) \in V \times Q_0$ , define the interpolant  $(\Pi_h^V u, \Pi_h^{Q_0} p_0) \in V_h \times Q_{0,h}$  as the unique **(A1)** solution of:

$$\begin{aligned}\langle 2\mu\varepsilon(\Pi_h^V u), \varepsilon(v) \rangle + \langle \Pi_h^{Q_0} p_0, \operatorname{div} v \rangle &= \langle 2\mu\varepsilon(u), \varepsilon(v) \rangle + \langle p_0, \operatorname{div} v \rangle \quad \forall v \in V_h, \\ \langle \operatorname{div} \Pi_h^V u, q_0 \rangle &= \langle \operatorname{div} u, q_0 \rangle \quad \forall q_0 \in Q_{0,h}.\end{aligned}$$

For any  $p_a \in Q_a$ , define the interpolant  $\Pi_h^{Q_a} p_a \in Q_{a,h}$  as the unique **(A2)** solution of:

$$\langle K_a \operatorname{grad} \Pi_h^{Q_a} p_a, q_a \rangle = \langle K_a \operatorname{grad} p_a, \operatorname{grad} q_a \rangle \quad \forall q_a \in Q_{a,h}.$$

For example, for Taylor-Hood type elements of order  $l$  (assuming elliptic regularity):

$$\begin{aligned}\|u - \Pi_h^V u\|_{H^1} + \|p_0 - \Pi_h^{Q_0} p_0\| &\lesssim h^m (\|u\|_{H^{m+1}} + \|p_0\|_{H^m}) \quad 1 \leq m \leq l+1, \\ \|p_a - \Pi_h^{Q_a} p_a\|_{H^1} &\lesssim h^m \|p_a\|_{H^{m+1}}, \quad \|p_a - \Pi_h^{Q_a} p_a\| \lesssim h^{m+1} \|p_a\|_{H^{m+1}} \quad 1 \leq m \leq l.\end{aligned}$$

Introduce decomposition into interpolation and discretization errors

$$e_u \equiv e_u^I + e_u^h, \quad e_u^I \equiv u - \Pi_h^V u, \quad e_u^h \equiv \Pi_h^V u - u_h;$$
$$e_{p_a} \equiv e_{p_a}^I + e_{p_a}^h, \quad e_{p_a}^I \equiv p_a - \Pi_h^{Q_a} p_a, \quad e_{p_a}^h \equiv \Pi_h^{Q_a} p_a - p_{a,h} \quad a = 0, \dots, A.$$

## Proposition (Discretization error estimate)

The *discretization errors* of the total pressure MPET approximations satisfy for  $t \in (0, T]$ :

$$\|e_{p_0}^h(t)\| + \|\varepsilon(e_u^h(t))\|_{2\mu} + \sum_{a=1}^A \|e_{p_a}^h(t)\|_{c_a} + \left( \int_0^t \sum_{a=1}^A \|\operatorname{grad} e_{p_a}^h\|_{K_a}^2 ds \right)^{\frac{1}{2}} + \dots$$
$$\lesssim E_0^h + \int_0^t \|\alpha \cdot e_p^I\|_{\lambda^{-1}} ds + \left( \int_0^t \sum_{a=1}^A \|c_a \dot{e}_{p_a}^I + S_j(e_p^I)\|^2 ds \right)^{\frac{1}{2}},$$

with implicit constant independent of  $h, T, \lambda, c_a$  and  $\xi_{a \leftarrow b}$  for  $a, b = 1, \dots, A$ , where  
 $E_0^h = \|\varepsilon(e_u^h(0))\|_{2\mu} + \sum_{a=1}^A \|e_{p_a}^h(0)\|_{c_a} + \|\alpha \cdot e_p^h(0)\|_{\lambda^{-1}}$ .

[Prop 4.1, ibid.]

Proof.

As for energy estimate using auxiliary interpolation estimates. □

## Theorem (Semi-discrete error estimate, Taylor–Hood-type elements)

Assume that  $(u, p)$  are sufficiently regular. For all  $t \in (0, T]$ , with implicit constants independent of  $h$ ,  $T$ ,  $\lambda$ ,  $c_j$  and  $\xi_{j \leftarrow i}$  for  $j, i = 1, \dots, J$ :

*First,*

$$\begin{aligned}\|u(t) - u_h(t)\|_{H^1} &\lesssim E_0^h + h^{l+1} (\|u(t)\|_{H^{l+2}} + \|u\|_{L^1(0,t;H^{l+2})} + \|p_0\|_{L^1(0,t;H^{l+1})}) \\ &\quad + \sum_{j=1}^J h^{l_j+1} (\|p_j\|_{L^1(0,t;H^{l_j+1})} + \|(\dot{p}_j, p_j)\|_{L^2(0,t;H^{l_j+1})}).\end{aligned}$$

*Second,*

$$\begin{aligned}\sum_{j=1}^J \|p_j - p_{j,h}\|_{L^2(0,t;H^1)} &\lesssim E_0^h + h^{l+1} (\|u\|_{L^1(0,t;H^{l+2})} + \|p_0\|_{L^1(0,t;H^{l+1})}) \\ &\quad + \sum_{j=1}^J h^{l_j} \|p_j\|_{L^2(0,t;H^{l_j+1})} + h^{l_j+1} (\|p_j\|_{L^1(0,t;H^{l_j+1})} + \|(\dot{p}_j, p_j)\|_{L^2(0,t;H^{l_j+1})}).\end{aligned}$$

*Third,*

$$\|p_0(t) - p_{0,h}(t)\| \lesssim h^{l+1} (\|p_0(t)\|_{H^{l+1}} + \|u(t)\|_{H^{l+2}}) + \|\varepsilon(e_u^h(t))\|_{2\mu}.$$

## Proof.

Discretization error estimate, Lagrange element interpolation estimates, Korn and Poincaré inequalities. □

# The total-pressure MPET formulation restores optimal convergence, including in the incompressible limit

Test case A with  
total-pressure  
augmented  
Taylor-Hood  
 $\mathcal{P}_2^d \times \mathcal{P}_1^{A+1}$   
discretization.

	$\ u - u_h\ _{L^\infty(0,T,L^2)}$	Rate	$\ u - u_h\ _{L^\infty(0,T,H^1)}$	Rate
$h$	$6.27 \times 10^{-2}$		$1.46 \times 10^0$	
$h/2$	$7.28 \times 10^{-3}$	3.11	$3.95 \times 10^{-1}$	1.88
$h/4$	$8.70 \times 10^{-4}$	3.06	$1.01 \times 10^{-1}$	1.97
$h/8$	$1.07 \times 10^{-4}$	3.02	$2.55 \times 10^{-2}$	1.99
$h/16$	$1.33 \times 10^{-5}$	3.01	$6.38 \times 10^{-3}$	2.00
Optimal		3		2

	$\ p_1 - p_{1,h}\ _{L^\infty(0,T,L^2)}$	Rate	$\ p_1 - p_{1,h}\ _{L^\infty(0,T,H^1)}$	Rate
$h$	$1.53 \times 10^{-1}$		$1.68 \times 10^0$	
$h/2$	$4.07 \times 10^{-2}$	1.91	$8.65 \times 10^{-1}$	0.96
$h/4$	$1.03 \times 10^{-2}$	1.98	$4.35 \times 10^{-1}$	0.99
$h/8$	$2.60 \times 10^{-3}$	1.99	$2.18 \times 10^{-1}$	1.00
$h/16$	$6.49 \times 10^{-4}$	2.00	$1.09 \times 10^{-1}$	1.00
Optimal		2		1

# The total-pressure MPET formulation restores optimal convergence, also for vanishing saturation coefficients

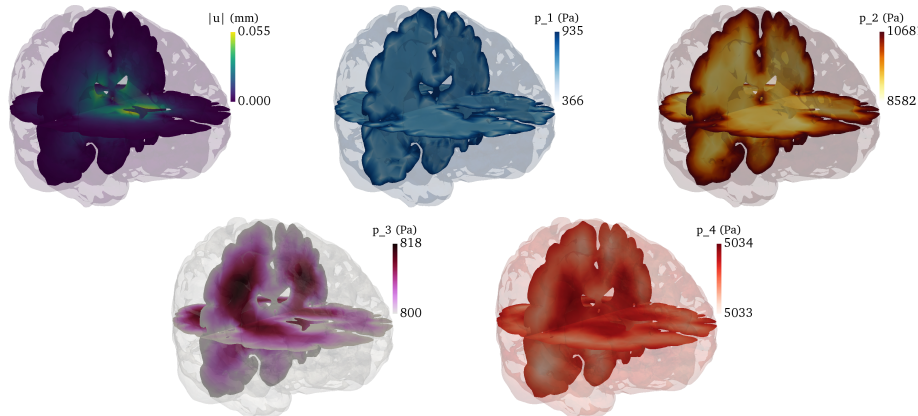
	$\ u - u_h\ _{L^\infty(0,T,L^2)}$	Rate	$\ u - u_h\ _{L^\infty(0,T,H^1)}$	Rate
$h$	$6.27 \times 10^{-2}$		$1.46 \times 10^0$	
$h/2$	$7.28 \times 10^{-3}$	3.11	$3.95 \times 10^{-1}$	1.88
$h/4$	$8.70 \times 10^{-4}$	3.06	$1.01 \times 10^{-1}$	1.97
$h/8$	$1.07 \times 10^{-4}$	3.02	$2.55 \times 10^{-2}$	1.99
$h/16$	$1.33 \times 10^{-5}$	3.01	$6.38 \times 10^{-3}$	2.00
Optimal		3		2

	$\ p_1 - p_{1,h}\ _{L^\infty(0,T,L^2)}$	Rate	$\ p_1 - p_{1,h}\ _{L^\infty(0,T,H^1)}$	Rate
$h$	$1.58 \times 10^{-1}$		$1.68 \times 10^0$	
$h/2$	$4.22 \times 10^{-2}$	1.90	$8.65 \times 10^{-1}$	0.96
$h/4$	$1.08 \times 10^{-2}$	1.97	$4.35 \times 10^{-1}$	0.99
$h/8$	$2.70 \times 10^{-3}$	1.99	$2.18 \times 10^{-1}$	1.00
$h/16$	$6.76 \times 10^{-4}$	2.00	$1.09 \times 10^{-1}$	1.00
Optimal		2		1

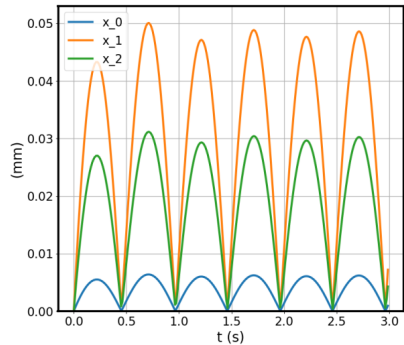
Test case A with  
total-pressure  
augmented  
Taylor-Hood  
 $\mathcal{P}_2^d \times \mathcal{P}_1^{A+1}$   
discretization but  
with  $c_a = 0$ .

# Are brain pulsations and extracellular fluid flow induced by arterial surface or bulk pulsations?

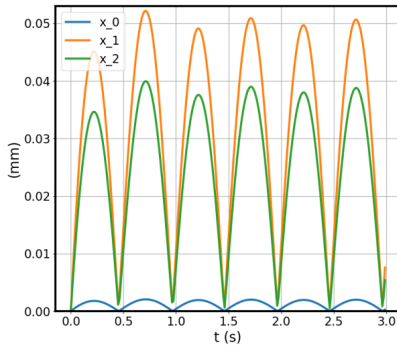


Slices of computed quantities at peak arterial inflow. From left to right and top to bottom: (a) displacement magnitude  $|u|$ , (b) extracellular pressure  $p_1$ , (c) arterial blood pressure  $p_2$ , (d) venous blood pressure  $p_3$  and (e) capillary blood pressure  $p_4$ .

# Displacements clearly differ between total pressure and standard mixed formulations ( $\nu = 0.4999$ )



(a) Total pressure formulation



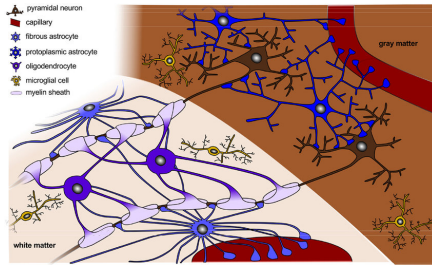
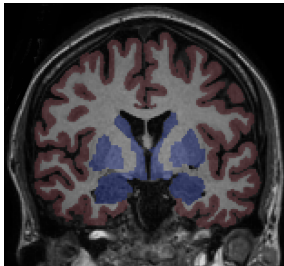
(b) 'Standard' formulation

Comparison of displacements computed using the standard and total pressure formulation. Plots of displacement magnitude  $|u(x_i, t)|$  versus time  $t$ , for a set of points  $x_0, x_1, x_2$ . The computed displacements clearly differ between the two solution methods

### **III: From hemispheres to brain meshes**

**Respecting gray and white matter**

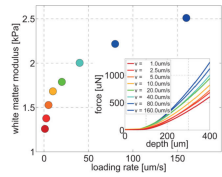
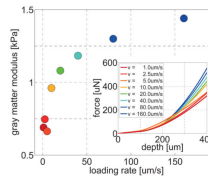
Gray and white matter differs substantially in terms of composition and biophysical properties



### Example:

Heterogeneous stiffness (permeability, diffusion) tensor

$$K = K(x) = \begin{cases} K_g & x \in \Omega_g \text{ (in gray matter),} \\ K_w & x \in \Omega_w \text{ (in white matter).} \end{cases}$$



[Budday et al (2015) (Fig 6), Budday et al (2019) (Fig 2)]

# Creating a mesh of gray and white matter from the surface segmentation

1. Convert FreeSurfer's pial and white left hemisphere surfaces to STL

```
$ mris_convert ./lh.pial pial.stl  
$ mris_convert ./lh.white white.stl
```

- 2 Create a mesh conforming to the interior interface using SVM-Tk
- 2 Include labels for the different regions relative to the surfaces

```
$ meshio-convert ernie-gw.mesh ernie-gw.vtu
```



Volume mesh of the left hemisphere conforming to the interior gray/white interface, and with the gray and white matter regions marked separately.

```
import SVMTK as svmtk

def create_gw_mesh(pial_stl, white_stl, output):
    # Load the surfaces
    pial = svmtk.Surface(pial_stl)
    white = svmtk.Surface(white_stl)
    surfaces = [pial, white]

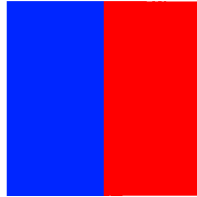
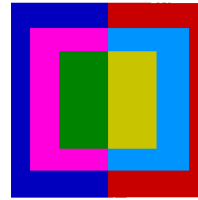
    # Create a map for the subdomains with tags
    # "1" is inside, "0" is outside
    # So: tag 1 for gray, 2 for white
    smap = svmtk.SubdomainMap()
    smap.add("10", 1)
    smap.add("11", 2)

    # Create a tagged domain from surfaces
    # and the map
    domain = svmtk.Domain(surfaces, smap)

    # Create and save the volume mesh
    resolution = 16
    domain.create_mesh(resolution)
    domain.save(output)

create_gw_mesh("lh.pial.stl", "lh.white.stl",
              "ernie-gw.mesh")
```

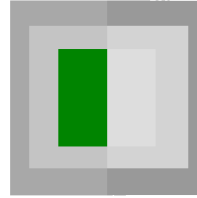
[Mandal et al (2021) (Chapter 4.1) ]

**A****B****C**

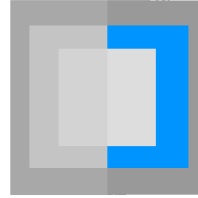
1000



0100



1011



0110

Colored squares representing subdomains enclosed by surfaces.

**Video example: Creating a gray and white matter mesh from surfaces**

## **Extracting the ventricular system**

The ventricular system is composed of four connected ventricles, connected through narrow passages and the subarachnoid space

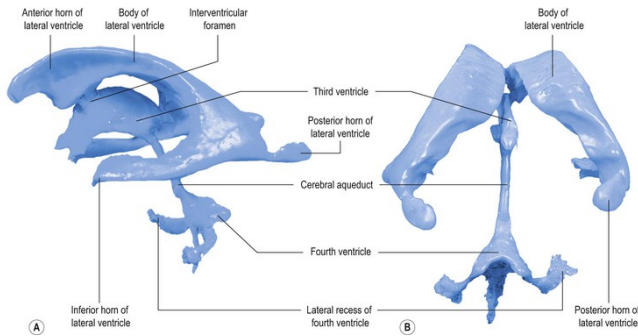
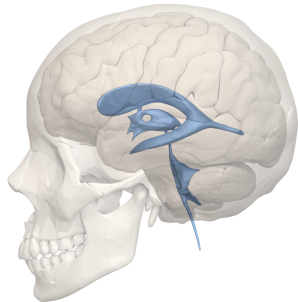
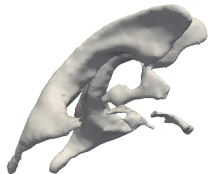


[Image from [neupsykey.com](http://neupsykey.com)]

# Extracting ventricular system surfaces from the segmentation



1. Mark voxels in the segmented images (aseg.mgz) matching given tags, and extract enclosing surface (mri\_binarize)
2. Improve the surface morphology by smoothing, extracting voxel clusters, .... (mri\_volcluster, mri\_morphology)
3. Remove ventricles during mesh generation using SVM-Tk

```
$ mri_binarize -help
```

```
...
# SVMTk Surfaces from STL files
surfaces = [pial, white, ventricles]
tags = {"pial":1, "white":2, "vent":3}

# Define the corresponding subdomain map
smap = svmtk.SubdomainMap()
smap.add("100", tags["pial"])
smap.add("110", tags["white"])
smap.add("111", tags["vent"])

# Mesh and tag the domain
domain = svmtk.Domain(surfaces, smap)
domain.create_mesh(32)

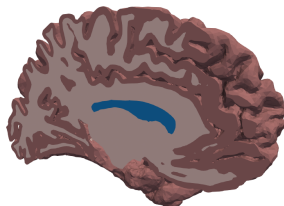
# Remove subdomain with given tag
domain.remove_subdomain(tags["vent"])
```

## **Video example: Extracting ventricular system surfaces**

## Combining hemispheres

# Joining the hemispheres to mesh the complete brain

- We combine the two pial surfaces, the union of the left and right white matter interface surface and the ventricular surface to generate a mesh of the whole brain.
- SVM-Tk allows for taking the union of surfaces.
- Chapter 4.3 of Mardal et al (2021) gives (much) more detail.



```
lhp, rhp = "lh.pial.stl", "rh.pial.stl"
lhw, rhw = "lh.white.stl", "rh.white.stl"
v = "ventricles.stl"

# Join the white surfaces
lhw.union(rhw)
surfaces = [lhp, rhp, lhw, v]

# Define identifying tags
tags = {"pial": 1, "white": 2, "vent": 3}

# Label the different regions
smap = svmtk.SubdomainMap()
smap.add("1000", tags["pial"])
smap.add("0100", tags["pial"])
...
.

# Generate mesh at given resolution
domain = svmtk.Domain(surfaces, smap)
domain.create_mesh(resolution)
domain.remove_subdomain(tags["vent"])
```

**Video example: combining and tagging hemispheres**

**Igor, bring me more brains!**

## Want to give it a try? Natural next steps:

1. Read Chapters 3-4 of [Mardal et al \(2021\)](#)
2. Try the scripts for generating meshes (gray/white, ventricles, joining hemispheres)
3. Examine your results in ParaView - do the markers and tags make sense? Are the boundaries/interfaces marked as expected?
4. Run a diffusion simulation with different diffusion coefficients in gray and white matter.
5. The source code associated with [Lee, Piersanti, Mardal, Rognes \(2019\)](#) is also available on Zenodo: <http://doi.org/10.5281/zenodo.1215636>. Try the MPET code on one of the brain meshes? (Caveat: we haven't run it in a few years...)